Electron Energy Bands in Tellurium*

R. E. BEISSNER†
Fort Worth Division of General Dynamics, Fort Worth, Texas
and
Texas Christian University, Fort Worth, Texas
(Received 10 December 1965)

The method of pseudopotentials was used to calculate the electron band structure of tellurium along the k_Z axis. The calculation was performed in two stages. First, a model pseudopotential, based on the free-atom data of Herman and Skillman, was used to compute a preliminary band structure. Perturbation theory was then used to estimate the changes in the band structure caused by corrections to the model pseudopotential. The calculated band structure shows a direct energy gap at the top of the Brillouin zone ($k_Z=\pi/c$) and an indirect gap of about the same magnitude between the valence band edge at $k_Z=0$ and the conduction band edge $k_Z=\pi/c$. It was found that s-p mixing is significant in the important valence and conduction bands. Because of this mixing, spin-orbit splitting, which was calculated in a second-order perturbation approximation, is much smaller than the corresponding splitting of the $5p$ free-atom level. The calculated band structure is consistent with the major features of the experimental infrared absorption spectrum including the 11-μ peak observed by Caldwell and Fan.

I. INTRODUCTION

SINCE 1954, when Loferski[1] first observed the polarization dependence of the fundamental optical absorption edge in single crystals of tellurium, there have been several attempts to construct an energy-band scheme which is consistent with such observed properties of the crystal.[2–5] Most of these investigations have been of a semiempirical nature in that they made use of symmetry-imposed restrictions on the degeneracies of the bands and then relied on experimental results or rough estimates of certain matrix elements in an attempt to deduce the ordering and spacing of the bands. Although the proposed band structures have some features in common, such as a minimum energy gap on the k_Z axis, there are important areas of disagreement. For example, Reitz's proposed band structure,[6] which is based on the tight-binding method, indicates that the minimum energy gap is at the top of the first Brillouin zone ($k_Z=\pi/c$), while Nussbaum and Hager,[3] who used the nearly-free-electron approach, suggest that the minimum gap is indirect, with conduction and valence band extrema near the center of the positive k_Z axis. Also, as might be expected, the over-all shapes of the energy bands deduced from the tight-binding and nearly-free-electron models are quite different. It was the existence of such uncertainties which prompted the present attempt to determine the band structure from more fundamental considerations.

The immediate objective of this work is, therefore, the calculation of the tellurium band structure along the k_Z axis with sufficient accuracy to determine the ordering of energy levels and, at least roughly, the spacing between levels. The calculated band structure should be adequate for the interpretation of the main features of the optical absorption spectrum and should provide qualitative information regarding the effective mass and density-of-states functions.

The choice of a calculation method was influenced by the demonstrated accuracy of the pseudopotential approach when applied to semiconductors of the diamond structure[7–9] and by the apparent success of several approximation schemes based on the idea of an atomic pseudopotential.[10] These investigations seem to support the contention that, as a first approximation, a valence electron in a metal or semiconductor may be treated as though it exists in the field of a periodic array of neutral, weakly attractive pseudo-atoms. Further, the band structure seems to be rather insensitive to "reasonable" approximations to the pseudopotential, i.e., the main features of the band structure seem to be determined to a large extent by the symmetry of the crystal. This last point is most clearly illustrated by the recent work of Falicov and Golin.[11] With these results in mind, the tellurium band structure was calculated in two steps. First, a preliminary structure was determined on the basis of a simplified atomic pseudopotential constructed from the free-atom wave functions of Herman and Skillman.[12] Spin-orbit effects were included by means of a second-order perturbation calculation. Next, first-order perturbation calculations were used to estimate the changes in the band structure

* Based on a dissertation submitted in partial fulfillment of the requirements for the degree of Doctor of Philosophy at Texas Christian University.

† Present address: Fort Worth Division of General Dynamics, Fort Worth, Texas.

[1] J. J. Loferski, Phys. Rev. **93**, 707 (1954).

[2] For a review of work prior to 1961, see J. S. Blakemore, D. Long, K. C. Nomura and A. Nussbaum, in *Progress in Semiconductors*, edited by A. F. Gibson (John Wiley & Sons, Inc., New York, 1961), Vol. 6.

[3] A. Nussbaum and R. J. Hager, Phys. Rev. **123**, 1958 (1961).

[4] M. Hulin, Ann. Phys. (Paris) **8**, 647 (1963).

[5] V. V. Sobolev, Dokl. Akad. Nauk SSSR **151**, 1308 (1963) [English transl.: Soviet Phys.—Dokl. **8**, 815 (1964)].

[6] J. R. Reitz, Phys. Rev. **105**, 1233 (1957).

[7] J. C. Phillips and L. Kleinman, Phys. Rev. **116**, 287 (1959).

[8] L. Kleinman and J. C. Phillips, Phys. Rev. **116**, 880 (1959).

[9] L. Kleinman and J. C. Phillips, Phys. Rev. **118**, 1153 (1960).

[10] J. Callaway, *Energy Band Theory* (Academic Press, Inc., New York, 1964), and references cited therein.

[11] L. M. Falicov and S. Golin, Phys. Rev. **137**, A871 (1965); S. Golin, Phys. Rev. **140**, A993 (1965).

[12] F. Herman and S. Skillman, *Atomic Structure Calculations* (Prentice-Hall, Inc., Englewood Cliffs, New Jersey, 1963).

induced by corrections to the pseudopotential. The perturbation calculations showed that such changes are small, thus justifying the use of a model pseudopotential. The final result is, therefore, an adjusted band structure which is qualitatively the same as the preliminary structure.

In Sec. II a brief review of the pseudopotential method is given. Section III contains a discussion of the tellurium crystal and its space group. The construction of an approximate crystal potential and pseudopotential is described in Sec. IV. In Sec. V a discussion is given of the calculated band structure, spin-orbit splitting, and the perturbation calculations used to adjust the preliminary structure. Finally, in Sec. VI the adjusted band structure is used to interpret certain infrared absorption measurements and is compared with recently published calculations for selenium,[13] which has the same crystal structure.

II. THE PSEUDOPOTENTIAL METHOD

The concept of a pseudopotential has its origin in a reformulation of the valence-state Schrödinger equation.[7] In its most general form, the pseudopotential theorem states that the valence-state equation,

$$(-\nabla^2+V(\mathbf{x}))\psi_{v\mathbf{k}}(\mathbf{x})=E_v(\mathbf{k})\psi_{v\mathbf{k}}(\mathbf{x}), \quad (1)$$

is equivalent to an effective wave equation,

$$(-\nabla^2+V(\mathbf{x})+V_R)\varphi_{v\mathbf{k}}(\mathbf{x})=E_v(\mathbf{k})\varphi_{v\mathbf{k}}(\mathbf{x}), \quad (2)$$

with

$$V_R=\sum_c|\psi_c\rangle\langle F_c|, \quad (3)$$

where $|\psi_c\rangle$ is a core state and $|F_c\rangle$ is an arbitrary vector.[14] It has been shown that the expectation value of V_R is positive, thus tending to cancel the expectation value of the attractive crystal potential V. This tendency to cancel means that the pseudopotential, $V+V_R$, is weaker than the actual crystal potential V. Thus the effective wave function $\varphi_{v\mathbf{k}}$ requires fewer terms in a plane-wave expansion than the actual wave function $\psi_{v\mathbf{k}}$. For this reason it has been suggested that the effective wave equation be used as a starting point for a plane-wave, linear-variational calculation of the valence-electron energies $E_v(\mathbf{k})$[7].

The arbitrariness of V_R implied by its definition suggests that the $|F_c\rangle$ be chosen so as to minimize the expectation value of the pseudopotential. Cohen and Heine[15] have shown that a near-optimum pseudopotential is

$$V(\mathbf{x})+V_R=(1-\sum_c|\psi_c\rangle\langle\psi_c|)V(\mathbf{x}),$$

which is obtained by taking $|F_c\rangle=-V(\mathbf{x})|\psi_c\rangle$. This form was used in the present calculations.

In practice, V_R is replaced by a local repulsive potential that is denoted by $V_{RL}(\mathbf{x})$. Thus,

$$V_{RL}(\mathbf{x})=-\sum_c\langle\psi_c|V|\varphi_{v\mathbf{k}}\rangle\psi_c(\mathbf{x})/\varphi_{v\mathbf{k}}(\mathbf{x}).$$

Phillips and Kleinman[7] have shown that if $\varphi_{v\mathbf{k}}$ may be approximated by a state of definite angular momentum l, in each atomic core, then V_{RL} reduces to the following spherically symmetric potential within each core:

$$V_{RL}{}^l(r)=-\sum_n\int_0^\infty P_{nl}(r')U_c(r')P_{vl}(r')dr'\frac{P_{nl}(r)}{P_{vl}(r)}, \quad (4)$$

where P_{nl} is the radial wave function for the core state with quantum numbers nl, $U_c(r)$ is the spherical average of the crystal potential in the core, and P_{vl} is the radial part of $\varphi_{v\mathbf{k}}$. If angular-momentum mixing is important, it has been suggested that V_{RL} be approximated by a linear combination of potentials of the form (4). In order to apply (4) it is, of course, necessary to introduce some additional assumptions regarding the behavior of the unknown function, $\varphi_{v\mathbf{k}}$, in the atomic core. Phillips and Kleinman have given arguments which indicate that, except for the l dependence implied in (4), the repulsive potential is rather insensitive to approximations to P_{vl}. Thus, the most serious uncertainty seems to lie in the assumption of a single angular-momentum state or a definite mixture of states. In subsequent sections of this paper, this problem will eb examined for the particular case of tellurium.

If one accepts the form (4) and makes the additional assumption that the crystal potential is a sum over all atom sites of a spherically symmetric potential $V(r)$, then the pseudopotential appearing in the effective wave equation (2) is just a sum over all sites of a spherically symmetric "atomic" pseudopotential. In this case the plane-wave matrix elements of the pseudopotential have the simple form

$$\langle\mathbf{k}|V+V_{RL}{}^l|\mathbf{k}+\mathbf{K}\rangle=S(\mathbf{K})V(|\mathbf{K}|),$$

where $|\mathbf{k}\rangle$ is a plane wave, $\mathbf{K}$ is a reciprocal lattice vector, $S(\mathbf{K})$ is the structure factor, and $V(|\mathbf{K}|)$ is the Fourier transform of the atomic pseudopotential, $V(r)+V_{RL}{}^l(r)$. Thus the introduction of an atomic pseudopotential simplifies the calculation of the matrix elements needed for a plane-wave, variational calculation of the band structure.

III. THE TELLURIUM CRYSTAL

The tellurium crystal structure is illustrated in Fig. 1. The Bravais lattice is hexagonal as shown in the upper half of the figure. The lower half shows how the nearest neighbors of an atom are located by screw operations along the C axis. The space group can be generated by combining the following symmetry operations with all lattice translations: (1) E, the identity; (2) C_3, a 120° rotation of the crystal about the C axis followed by a translation $C/3$ along the axis; (3) $C_3{}^2$; (4) $C_2{}^{(1)}$, a 180° rotation about the $X^{(1)}$ axis followed by a translation

[13] D. J. Olechna and R. S. Knox, Phys. Rev. **140**, A986 (1965).
[14] B. J. Austin, V. Heine and L. J. Sham, Phys. Rev. **127**, 276 (1962).
[15] M. H. Cohen and V. Heine, Phys. Rev. **122**, 1821 (1961).

TABLE I. Double group character table for the group of $\mathbf{k}$ on the k_Z axis of tellurium. T is a 2π rotation, $\epsilon=\exp(2\pi i/3)$, $\delta=\exp(-ik_ZC/3)$, and $\nu_\pm$ are the spin up (+) and spin down (−) functions.

Representation	E	C_3	C_3^2	TE	TC_3	TC_3^2	Basis
Δ_1	1	δ	δ^2	1	δ	δ^2	Δ_1
Δ_2	1	$\epsilon\delta$	$\epsilon^*\delta^2$	1	$\epsilon\delta$	$\epsilon^*\delta^2$	Δ_2
Δ_3	1	$\epsilon^*\delta$	$\epsilon\delta^2$	1	$\epsilon^*\delta$	$\epsilon\delta^2$	Δ_3
Δ_4	1	$-\epsilon^*\delta$	$\epsilon\delta^2$	−1	$\epsilon^*\delta$	$-\epsilon\delta^2$	$\Delta_1\nu_-$, $\Delta_2\nu_+$
Δ_5	1	$-\epsilon\delta$	$\epsilon^*\delta^2$	−1	$\epsilon\delta$	$-\epsilon^*\delta^2$	$\Delta_1\nu_+$, $\Delta_3\nu_-$
Δ_6	1	$-\delta$	δ^2	−1	δ	$-\delta^2$	$\Delta_2\nu_-$, $\Delta_3\nu_+$

$C/3$; (5) $C_2^{(2)}$, a 180° rotation about $X^{(2)}$; (6) $C_2^{(3)}$, a 180° rotation about $X^{(3)}$ followed by a translation $2C/3$. The operations are defined with the point transformation convention and the notation adopted by Blakemore *et al.*[2].

The first Brillouin zone is a right hexagonal prism centered at $\mathbf{k}=0$ with bases parallel to the x-y plane of Fig. 1 at $k_Z=\pi/C$. The double-group characters for the group of the wave vector on the k_Z axis are given in Table I. The representations Δ_1, Δ_2, and Δ_3 are formed from spin-independent basis functions; Δ_4, Δ_5, and Δ_6 are the extra representations whose bases are the spin-independent functions shown in the right-hand column. For more details concerning the tellurium space group and its representations, the reader is referred to Asendorf's article.[16]

IV. CALCULATION OF THE PSEUDOPOTENTIAL

Previous studies of the cancellation of the crystal and repulsive potentials have shown that the net potential (the pseudopotential) is quite sensitive to approximations to the core functions. In fact, the work of Kleinman and Phillips[9] suggests that, given a realistic crystal potential, the band structure is more sensitive to approximations to the core eigenfunctions than it is to the choice of the crystal potential itself. Thus, if one is given a set of core functions which are eigenfunctions of an approximate crystal Hamiltonian, it may be better to construct a pseudopotential on the basis of the information given than to use approximate core eigenfunctions of a more accurate Hamiltonian. The calculations described below, therefore, started with the assumption that the core functions are Bloch sums of the free-atom orbitals computed by Herman and Skillman. Next, a crystal potential which is consistent with this assumption was chosen, thus providing the information necessary for the determination of an approximate pseudopotential.

Figure 2 shows the Herman-Skillman and Thomas-Fermi screening functions, which are defined as

$$f(r)=-(r/2Z)V(r),$$

where $V(r)$ is the atomic potential. The Thomas-Fermi

[16] R. H. Asendorf, J. Chem. Phys. **27**, 11 (1957).

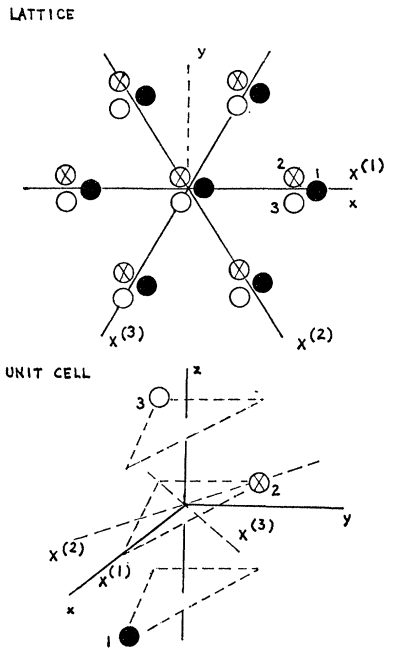

FIG. 1. The tellurium crystal.

potential is the less attractive of the two because it is a neutral-atom potential, while the Herman-Skillman potential is that of a bound atomic electron. In the core ($r<2$ Bohr radii), however, there is not much difference between the two functions because the potential in the core is dominated by the strongly attractive contribution of the core itself.

In a crystal, one effect of neighboring atoms is to make the potential more attractive everywhere, but, in the core of a high-Z atom such as tellurium, this additional attractive potential should be small compared to the atomic-core potential. For this reason, the calculation was started with the tentative assumption that, in the core, the effect of neighboring atoms in the tellurium crystal is just enough to make up the small difference between the Thomas-Fermi and Herman-Skillman potentials. In other words, the assumption was that a crystal potential which is consistent with the choice of Herman-Skillman wave functions can be constructed by summing the Thomas-Fermi potential over all atom sites. This assumption was tested by calculating the spherical average

$$U_c(r)=\frac{1}{4\pi r^2}\int_0^{2\pi}\int_0^{\pi}V(r,\theta,\varphi)r^2\sin\theta d\theta d\varphi,$$

where $V(r,\theta,\varphi)$ is the approximate crystal potential obtained by summing the Thomas-Fermi atomic potential over an atom at the origin and its first, second, and third nearest neighbors. In the core, U_c differed from the Herman-Skillman potential by less than 5%, which is within the accuracy of the spherical average approximation, thus justifying the use of the Thomas-Fermi crystal potential with Herman-Skillman core functions.

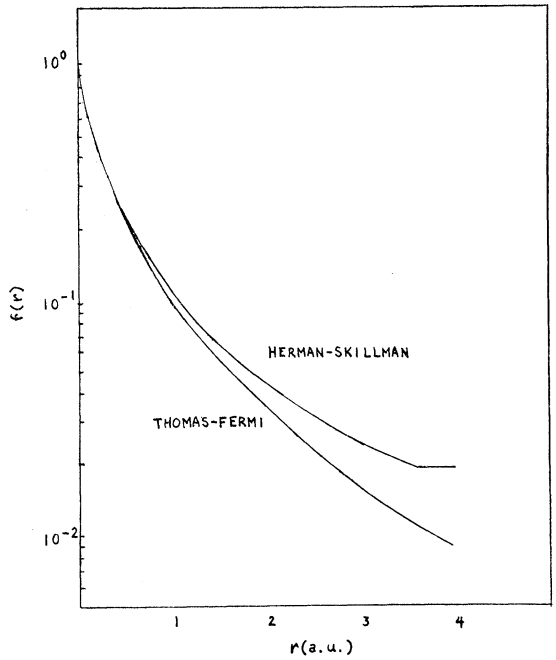

FIG. 2. The Thomas-Fermi and Herman-Skillman screening functions for tellurium. The functions plotted are $f(r) = -(r/2Z)V(r)$ where $V(r)$ is the atomic potential. r is in atomic units.

The Thomas-Fermi model of the crystal potential is, of course, an oversimplification for the region between atomic cores where exchange and crystalline field effects are known to be important. On the other hand, the potential should be quantitatively accurate in the core, and provides at least a qualitative description of the potential outside the core. Thus, the Thomas-Fermi potential was used as a semiquantitative model, subject to an empirical correction for its inaccuracy outside the core. This empirical correction is discussed in Sec. V.

To construct a repulsive potential V_{RL} it is necessary to introduce some assumptions regarding the l dependence of $\varphi_{v\mathbf{k}}$, as noted in Sec. II. If one were to follow the suggestion of Phillips and Kleinman, it would be necessary to compute a repulsive potential which is a linear combination of the $V_{RL}{}^l$:

$$V_{RL}(\mathbf{x}) = \sum_l \omega_l(\mathbf{k},v) V_{RL}{}^l(\mathbf{x}),$$

where the sum is over all angular momenta included among the core states. For tellurium, $l=0$, 1, 2. To avoid the complications associated with the calculation of the ω_l, which may vary from point to point within the Brillouin zone, it was assumed that, as a first approximation, $\varphi_{v\mathbf{k}}$ could be considered a pure p state for all bands of interest and that the effects of any angular-momentum mixing which may exist are small enough to be treated by perturbation theory. Thus it was assumed that $\omega_0=\omega_2=0$ and $\omega_1=1$, so that the repulsive potential was given by (4) with $l=1$. The Herman-Skillman wave functions and potential were used for P_{nl} and U_c, respectively. The integrals appearing in (4) involve the unknown function P_{vl} and so were approximated by the procedure given below.

From (1), (2), and (3) it is easily verified that the actual wave function is given by

$$\psi_{v\mathbf{k}} = \varphi_{v\mathbf{k}} - \sum_\alpha \frac{\langle F_\alpha | \varphi_{v\mathbf{k}} \rangle}{E_v(\mathbf{k}) - E_\alpha} \psi_\alpha. \tag{5}$$

Therefore,

$$\langle F_c | \psi_{v\mathbf{k}} \rangle = \langle F_c | \varphi_{v\mathbf{k}} \rangle - \sum_\alpha \frac{\langle F_\alpha | \varphi_{v\mathbf{k}} \rangle}{E_v(\mathbf{k}) - E_\alpha} \langle F_c | \psi_\alpha \rangle$$

$$= \sum_\alpha \left[\delta_{c\alpha} - \frac{\langle F_c | \psi_\alpha \rangle}{E_v(\mathbf{k}) - E_\alpha} \right] \langle F_\alpha | \varphi_{v\mathbf{k}} \rangle. \tag{6}$$

The set of Eqs. (6) was solved for the unknown quantities $\langle F_c | \varphi_{v\mathbf{k}} \rangle$, which are the integrals appearing in (4), by taking $F_c = -V\psi_c$, approximating E_v and E_c by the Herman-Skillman atomic term values, and assuming that $\psi_{v\mathbf{k}}$ reduces to the Herman-Skillman $5p$ function in the core. Substitution in (5) determined $\varphi_{v\mathbf{k}}$ and, hence, its radial part P_{vl}. The p-state pseudopotential was then computed according to (4). Figure 3 shows the Fourier transforms of the Thomas-Fermi potential and the p-state "atomic" pseudopotential. This illustrates the expected result: partial cancellation of the crystal potential and the repulsive potential yields a pseudopotential which is generally attractive and much weaker than the crystal potential.

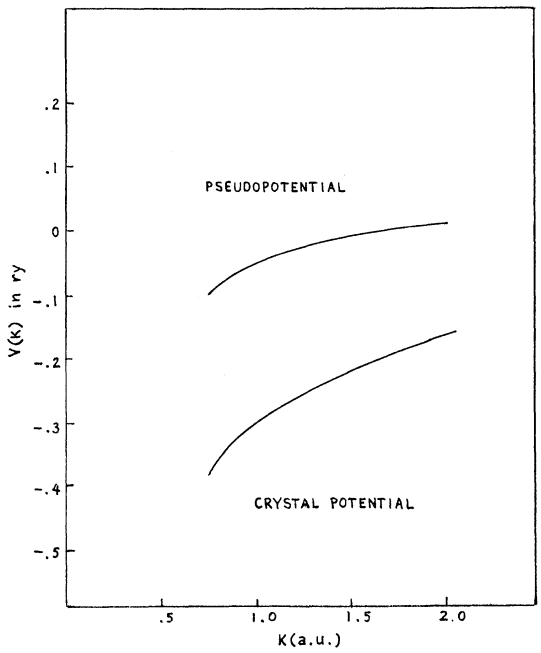

FIG. 3. Fourier transforms of the crystal potential and pseudopotential. The functions illustrated here are to be multiplied by the tellurium structure factor.

V. BAND STRUCTURE CALCULATIONS

The electron energy levels on the k_Z axis were calculated in the usual way by taking φ_{vk} to be a linear combination of plane waves, applying the variational principle, and solving the resulting secular equations for the energies at particular values of $\mathbf{k}$. Plane-wave expansions of 16, 22, and 29 terms were used and eigenvalues were calculated at $k_Z=0$, $\pi/2C$, and π/C. Because there are only three irreducible representations on the k_Z axis and the representations are nondegenerate, the 29-term approximation involved 9×9 and 10×10 determinants. The decision to stop the calculation at 29 terms was based on three observations. First, there was no change in the ordering of the levels and no significant change in the over-all structure, including the magnitude of the minimum energy gap, in going from 22 to 29 terms. Second, the calculation was based on a pure p-state pseudopotential and was to be corrected for the effects of $l\neq1$ terms. Finally, the addition of more plane-wave terms would not have introduced any additional strong coupling with the most important plane-wave terms. By this it is meant that the potential-energy matrix elements between any additional terms and the 16 plane waves which determine a first approximation to the band structure would have involved $V(K)$ at large values of K ($K>1.4$ Bohr radii^{-1}); the 29-term approximation included all plane waves which are coupled to the original 16 waves through small values of K. Thus the addition of more terms would have resulted in smaller changes in the band structure than were observed in going from 22 to 29 terms.

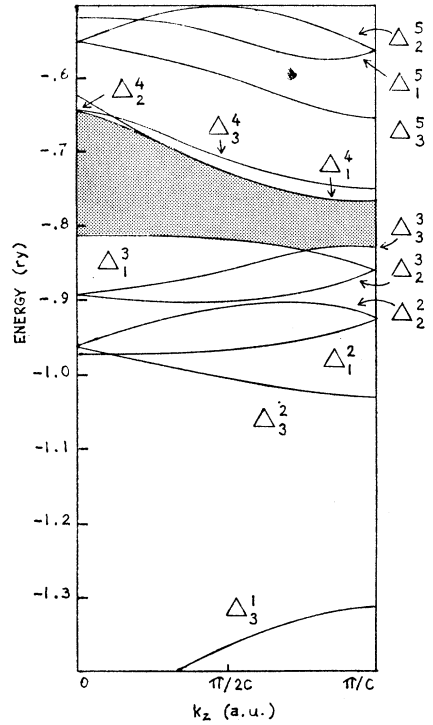

FIG. 4. Calculated band structure without spin-orbit splitting. The irreducible representations are defined in Table I. Superscripts are used to distinguish bands of the same symmetry.

The calculated band structure is plotted in Fig. 4. Bands of the same symmetry are distinguished from one another by a superscript which denotes the ordering of the levels; the shaded area represents the gap between conduction and valence bands. It is worth noting that, in spite of the approximations involved in the construction of the pseudopotential, the minimum energy gap is of the right order of magnitude. Both the direct gap between Δ_3^3 and Δ_1^4 at $k_Z=\pi/C$ and the indirect gap between Δ_1^3 at $k_Z=0$ and Δ_1^4 at $k_Z=\pi/C$ have the same value ($E_{\text{gap}}\approx0.065$ Ry) within the accuracy of the calculation. The experimental gap[2] is 0.024 Ry. Also, the existence of a direct gap between states of different symmetry is consistent with observed properties of the fundamental absorption edge, as shown in Sec. VI. Finally, the accidental degeneracy of Δ_1^3 and Δ_3^3 near $k_Z=\pi/C$ leads to an explanation for the polarization-dependent absorption peak reported by Caldwell and Fan.[17] This point is also discussed in Sec. VI. Thus the band structure shown in Fig. 4 is consistent with experiment. The task which remains is to demonstrate that this consistency is not upset by the effects of spin-orbit splitting or by corrections to the pseudopotential.

As Table I shows, the spin-orbit interaction removes the two-fold spin degeneracy of all states on the k_Z axis. The splitting was calculated using the approximation introduced by Liu,[18]

$$\langle\psi_{sk}|H_1|\psi_{vk}\rangle\approx\sum_c\langle\psi_c|H_1|\psi_c\rangle\langle\varphi_{sk}|\psi_c\rangle\langle\psi_c|\varphi_{vk}\rangle,$$

where H_1 is the spin-orbit operator, ψ_{vk}, φ_{vk}, and ψ_c are the spin-dependent analogs of the functions defined in Sec. II, and the sum is over all core states including spin. The matrix elements were calculated using the spin-orbit energies, $\langle\psi_c|H_1|\psi_c\rangle$, computed by Herman and Skillman and neglecting d-state contributions, which are an order of magnitude smaller than the p-state energies.[12] The linear combinations of plane waves determined by the spin-independent variational calculation were used in computing the integrals $\langle\varphi_{vk}|\psi_c\rangle$. The result of a second-order perturbation calculation, which included interactions among the unperturbed Δ^2, Δ^3, and Δ^4 bands, is summarized in Fig. 5. It can be seen that the splitting is quite small for most bands. In fact, the calculated spin-orbit energies are at least a factor of 2 smaller than the corresponding $5p$ energy shifts for the free atom computed by Herman and Skillman. For most bands, the calculated splitting was less than 0.005 Ry and was too small to estimate.

The surprisingly small spin-orbit energies were interpreted as an indication that there is much more s-p and p-d mixing in the valence states than was

[17] R. S. Caldwell and H. Y. Fan, Phys. Rev. **114**, 664 (1959).
[18] L. Liu, Phys. Rev. **126**, 1317 (1962).

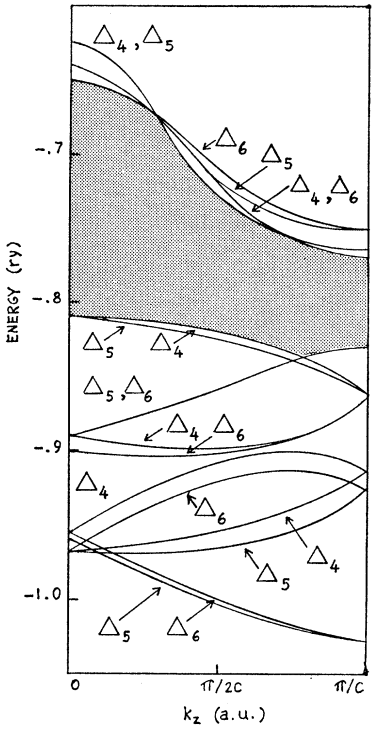

FIG. 5. Calculated band structure with spin-orbit splitting.

originally anticipated.[19] This explanation was confirmed, in part, by comparisons of some of the integrals, $\langle\varphi_{vk}|\psi_c\rangle$, for s and p states. For example, the ratio of the s-state occupation probability to the p-state probability is 1.27 for Δ_1^3 at $k_Z=\pi/C$, and the corresponding ratio for Δ_2^2 at $k_Z=\pi/C$, where the splitting is significant, is 0.005. Thus it is clear that there is considerable mixing of angular-momentum states in φ_{vk} and that the extent of this mixing varies markedly from state to state. This means that the assumption of a pure p-state pseudopotential was an oversimplification; the repulsive-potential operator defined in Sec. II should have been replaced by a rather complicated mixture of the $V_{RL}{}^l$ for $l=0$, 1, 2. On the other hand, if the band structure is as insensitive to errors in the pseudopotential as expected, the introduction of a more accurate and more complicated expression for the repulsive potential should result in only small changes in the band structure. For this reason, the difference between the exact operator, V_R, and the local approximation, $V_{RL}{}^1$, was treated as a perturbation, the variationally determined band structure and wave functions being the unperturbed quantities.

The corrections applied to the calculated band structure were

$$\Delta E_v(\mathbf{k})=\langle\varphi_{vk}|\,V_R-V_{RL}{}^1(\mathbf{x})\,|\varphi_{vk}\rangle.$$

[19] In their linear combination of atomic orbitals study of selenium, which was published after the present calculations had been concluded, Olechna and Knox (Ref. 13) found the s-p hybridization had a pronounced effect on the band structure. Thus, their results provide a strong indication that s-p mixing is also significant in the valence states of tellurium.

Following Phillips and Kleinman,[7] φ_{vk} was expanded in spherical waves,

$$\varphi_{vk}(\mathbf{x})=\sum_{l=0}^{\infty}\varphi_{vk}{}^l(\mathbf{x}),$$

and V_R was rewritten as a sum over the core angular momentum states,

$$V_R=\sum_{l=0}^{2}V_R{}^l.$$

From the definition of V_R given in Sec. II, it is easily verified that

$$V_R\varphi_{vk}(\mathbf{x})=\sum_{l=0}^{2}V_R{}^l\varphi_{vk}{}^l(\mathbf{x})$$

if the crystal potential is assumed to be spherically symmetric in the core. Also, because $V_{RL}{}^1(\mathbf{x})$ is spherically symmetric in each core,

$$\langle\varphi_{vk}|\,V_{RL}{}^1|\,\varphi_{vk}\rangle=\textstyle\sum_l\langle\varphi_{vk}{}^l|\,V_{RL}{}^1|\,\varphi_{vk}{}^l\rangle.$$

Therefore,

$$\begin{aligned}\Delta E_v(\mathbf{k})&=\textstyle\sum_l\langle\varphi_{vk}{}^l|\,V_R{}^l-V_{RL}{}^1|\,\varphi_{vk}{}^l\rangle\\&\approx\textstyle\sum_l\langle\varphi_{vk}{}^l|\,V_{RL}{}^l-V_{RL}{}^1|\,\varphi_{vk}{}^l\rangle\\&\approx\langle\varphi_{vk}{}^0|\,V_{RL}{}^0-V_{RL}{}^1|\,\varphi_{vk}{}^0\rangle\\&\quad+\langle\varphi_{vk}{}^2|\,V_{RL}{}^2-V_{RL}{}^1|\,\varphi_{vk}{}^2\rangle\\&\quad-\sum_{l=3}^{\infty}\langle\varphi_{vk}{}^l|\,V_{RL}{}^1|\,\varphi_{vk}{}^l\rangle.\end{aligned}$$

The last term, which is a correction for the presence of $l>2$ terms in φ_{vk}, was not considered in computing $\Delta E_v(\mathbf{k})$. The s and d repulsive potentials were calculated according to (4) with the approximation

$$P_{vl}(r)\approx rj_l(r),$$

where $j_l(r)$ is the spherical Bessel function. This approximation was based on the observation that $|\mathbf{k}+\mathbf{K}|\approx1$ for the dominant terms in the plane-wave expansion of φ_{vk}. The $\Delta E_v(\mathbf{k})$ were calculated at $k_Z=0$ and $k_Z=\pi/C$ for the Δ^3 and Δ^4 bands of Fig. 4. It was found that the correction was too small ($\Delta E_v<0.01$ Ry) to require a reordering of the levels. This result is encouraging in one sense, for it shows that the main features of the band structure are insensitive to the variations of the pseudopotential that result from variations of the mixtures of s, p, and d states in φ_{vk}.

However, the mixing corrections failed to produce a significant change in the predicted energy gap, which is too large by more than a factor of 2. As was noted earlier, the magnitude of the energy gap did not change much as the order of approximation was increased in the variational calculation of the energy bands. Thus it did not seem likely that the failure to predict the correct gap was due to convergence difficulties. Rather, it was concluded that the poor prediction was due to

an inadequate approximation to the crystal potential, particularly in the region between atomic cores where the Thomas-Fermi theory is least accurate. Therefore, at this point, the remaining problem was to determine whether or not a physically plausible adjustment of the Thomas-Fermi crystal potential could be found such that the correct energy gap is produced without causing drastic alterations of the calculated band structure.

From the perturbation calculations described earlier, it was evident that the minimum energy gap could be narrowed by adjusting the pseudopotential so that it is more attractive outside the core. Such an adjustment might be attributed to the addition of an exchange potential, which is attractive and is usually significant outside the core.[20] To see how a more attractive crystal potential would affect the over-all band structure, the Fourier transform of the pseudopotential was arbitrarily altered, as shown in Fig. 6. First-order perturbation corrections were then computed at selected points on the energy bands. The significant results are:

1. The energy gap was narrowed, as expected, by increasing the energy of Δ_3^3 and decreasing the energy of Δ_1^4 at $k_Z=\pi/C$. It happened that the arbitrarily adjusted pseudopotential shown in Fig. 6 produced the correct gap.

2. The Δ_1^3 level at $k_Z=\pi/C$ was lowered substantially. In fact, the computed energy shift was too large to be meaningful in a first-order perturbation treatment.

3. The Δ_1^3 band was raised near $k_Z=0$ so that the direct and indirect gaps have about the same value.

4. The level at Δ_3^4, $k_Z=\pi/C$ was raised, thus increasing the gap between Δ_1^4 and Δ_3^4.

Of course, these perturbation calculations have only qualitative significance. The important point is that it was possible to adjust the pseudopotential so as to obtain the correct energy gap without changing the ordering and general shapes of the energy bands shown in Fig. 4.

VI. COMPARISON WITH EXPERIMENT

The selection rules for electric dipole transitions between bands on the k_Z axis have been reported by Hulin[4] and are summarized in Table II. The symbols σ and π refer to the polarization of the radiation, σ meaning that the electric field vector is parallel to the C axis of the crystal ($E\|C$) and π meaning $E\perp C$. An allowed electric dipole transition is indicated by the symbol denoting the polarization. It can be shown that magnetic dipole transitions can occur in all situations where electric dipole transitions are forbidden.

TABLE II. Selection rules for electric dipole transitions between states on the k_Z axis.

Initial state	Final state Δ_1	Δ_2	Δ_3
Δ_1	σ	π	π
Δ_2	π	σ	π
Δ_3	π	π	σ

[20] Olechna and Knox (Ref. 13) have demonstrated that, for selenium, the introduction of an exchange potential does indeed narrow the energy gap. They have also shown that with a physically reasonable choice of the exchange potential, the predicted gap is in good agreement with experiment.

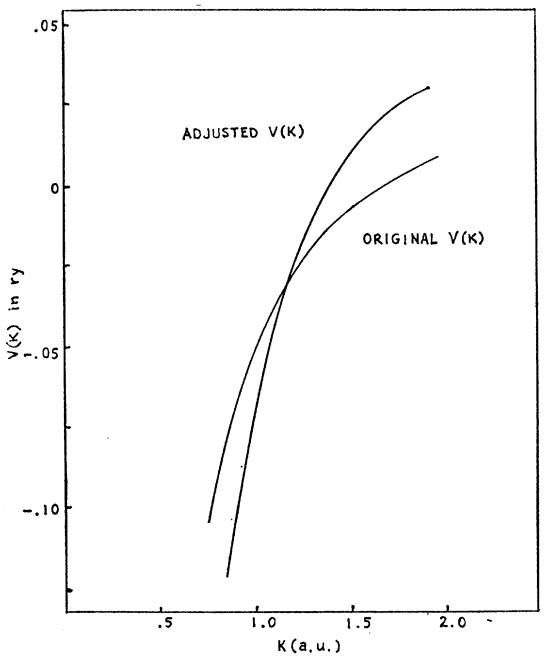

FIG. 6. Fourier transform of the adjusted pseudopotential. This adjustment was used to obtain estimates of the sensitivity of the band structure to changes in the pseudopotential.

Experimental investigations by Loferski[1] and, more recently, by Blakemore and Nomura[21] and by Sobolev[5] show that the infrared absorption coefficient corresponding to the excitation of electrons across the energy gap is much larger for π radiation than for σ radiation. According to the selection rules discussed above, this result implies that the valence and conduction band edges belong to different irreducible representations. The calculated band structure indicates that both direct and indirect transitions are involved in the absorption process. However, because indirect transitions are nominally forbidden, the polarization dependence of the absorption coefficient should be dominated by direct transitions from Δ_3^3 to Δ_1^4 at $k_Z=\pi/C$, which is in agreement with the experimental result.[22]

Caldwell and Fan[17] have observed an absorption peak at a photon wavelength of 11 μ ($\approx$0.007 Ry) with incident σ radiation; it was not observable with π radiation. The temperature sensitivity of the peak indicates that it is associated with transitions of holes from one valence band to another. Because the peak is observed at low temperatures, the valence bands

[21] J. S. Blakemore and K. C. Nomura, Phys. Rev. **127**, 1024 (1962).

[22] Spin-orbit splitting is negligible in this case. Thus the spin-independent structure of Fig. 4 is used.

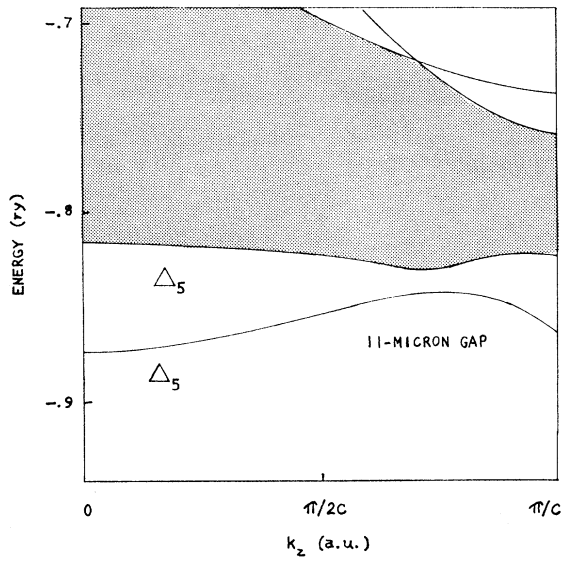

FIG. 7. Detail from Fig. 5 showing the proposed origin of the 11-μ absorption peak. It is suggested that a detailed calculation of the spin-orbit effect at the point of intersection of Δ_1^3 and Δ_3^3 would result in the removal of the apparent degeneracy of the corresponding Δ_5 bands, thus producing the gap sketched above.

involved must be near the valence band edge. Thus, the data imply that there are two valence bands of the same symmetry, separated by a small gap and lying near the maximum valence-band energy. The structure shown in Fig. 5 suggests that the peak is a result of transitions between the two Δ_5 bands that appear to cross near $k_Z=\pi/C$. The removal of this apparent degeneracy by a more complete treatment of the spin-orbit effect would result in a small gap between the Δ_5 bands, as sketched in Fig. 7. If the Δ_1^3 and Δ_3^3 bands cross, as Fig. 4 and the supporting pseudopotential correction study indicate, then the existence of such a small gap is assured. However, the position and magnitude of the gap remains uncertain because the calculation of those features requires a detailed knowledge of the Δ_1^3 and Δ_3^3 wave functions near the gap. The perturbation calculations of Sec. V show that the Δ_3^3 function is sensitive to errors in the pseudopotential in that region.

Recent calculations of the selenium band structure by Olechna and Knox[13] make possible some interesting observations concerning the selenium and tellurium absorption spectra. In comparing the present tellurium band structure with the selenium results reported by Olechna and Knox, it should be noted that, because of the point transformation convention used in the present paper, the symbols Δ_2 and Δ_3 should be interchanged. According to the Olechna-Knox calculations the selenium Δ_3^3 band (in the notation of the present paper) lies below the Δ_1^3 and Δ_2^3 bands. In tellurium the Δ_3^3 band crosses Δ_1^3 and forms the valence band edge at $k_Z=\pi/C$. Therefore, in selenium, the transitions corresponding to the fundamental absorption edge are allowed with σ radiation while in tellurium the allowed transitions occur with π radiation. Also, because the Δ_1^3 and Δ_3^3 bands do not cross in selenium, there is no gap comparable to the 11-μ gap in tellurium. Thus it seems that the major differences between the selenium and tellurium absorption spectra are explained by the Olechna-Knox calculations for selenium and the present calculations for tellurium.

VII. SUMMARY AND CONCLUSIONS

The method of pseudopotentials has been applied to a study of the tellurium band structure along the k_Z axis. It has been shown that the main features of the energy bands are insensitive to small errors in the pseudopotential, thus justifying the use of a simplified crystal potential and a p-state atomic pseudopotential. The calculated band structure is consistent with infrared absorption data and, in view of the rather rough treatment of the crystal potential, gives a reasonably accurate prediction of the energy gap. The correct gap can be produced by making the model pseudopotential more attractive between atomic cores. The calculations also show that there is considerable s-p and possibly p-d mixing in the important valence and conduction states and that the extent of this mixing is strongly dependent on the state. Although corrections for the presence of mixed states do not alter the qualitative features of the energy bands in the absence of a spin-orbit interaction, mixing effects are responsible for the spin-orbit splitting being much smaller than the assumption of pure p bands would suggest.

It is evident that the success of the present calculation depends strongly on the insensitivity of the band structure to small errors in the pseudopotential. The origin of this insensitivity is well-known. The crystal and repulsive potentials cancel each other to such an extent that the Hamiltonian matrix is dominated by the diagonal kinetic-energy terms. It is therefore expected that small errors in the weakly attractive pseudopotential result in even smaller errors in the band structure, regardless of the crystal structure and the presence of angular-momentum mixing in the valence states. Nevertheless, it is encouraging to note that this effect has now been demonstrated by actual calculation for the tellurium structure, as well as cubic structures, for a case where s-p-d mixing leads to significant uncertainties in the pseudopotential.

ACKNOWLEDGMENTS

The author wishes to thank Professor H. M. Moseley for several valuable discussions, Dr. A. A. J. Hoffman and the staff of the TCU Computer Center for their assistance in performing the calculations and Dr. E. L. Secrest, Dr. J. C. Redmond, Dr. J. N. Silverman, and Dr. B. C. Deaton for helpful suggestions.